Flux-charge duality and quantum phase fluctuations in one-dimensional superconductors

Andrew J. Kerman

MIT Lincoln Laboratory, Lexington, MA, USA

(Dated: January 26, 2023)

It has long been thought that superconductivity breaks down even at zero temperature in lower-dimensional systems due to enhanced quantum phase fluctuations. In 1D wires, these fluctuations are described in terms "quantum phase-slip" (QPS): tunneling of the superconducting order parameter between states whose relative phase differs by $\pm 2\pi$. Although many phenomena observed experimentally in narrow superconducting wires over the last several decades have been attributed to QPS, such as anomalous resistive fluctuations and even a complete destruction of superconductivity in the narrowest wires, a clear and unifying understanding has not yet been achieved. In this article we present a new theory for QPS based on the idea that flux-charge duality, a classical symmetry of Maxwell's equations, relates the phase fluctuations associated with QPS to the well-known charge fluctuations associated with Josephson tunneling, at a microscopic level. This theory successfully explains many phenomena observed in experiments, and also provides a conceptual link to quantum phase fluctuations in 2D superconductors.

PACS numbers: Valid PACS appear here

Phase fluctuations are one of the important ways that mean-field theories of superconductivity break down in lower-dimensional systems, such as lattice planes in high-T_C superconductors [1, 2], thin films [3–5], and narrow wires [6]. In quasi-1D wires, they come in the form of "phase slips": topological excitations in which the phase difference ϕ between the wire's ends changes by $\pm 2\pi$. Such a process was first suggested by Little [7], in which thermal energy causes a short segment of the wire to fluctuate into the normal state, allowing ϕ to "slip" by one cycle. This was later treated by Langer, Ambegaokar, McCumber, and Halperin (LAMH) [8] and others [9] as a source of finite resistance just below the critical temperature T_C, and subsequent experiments [10] on $\sim$0.2-0.5 μm-diameter crystalline Sn "whiskers" validated these ideas.

In 1986, by analogy to macroscopic quantum tunneling in Josephson junctions (JJs) [11], Mooij and co-workers proposed that for narrow enough wires, a *quantum* phase slip (QPS) process might be observable, in which the superconductor *tunnels* between states whose phase differs by $\pm 2\pi$ [12]. Shortly thereafter, using lithographically defined, $\sim$ 50 nm-wide In wires, Giordano measured finite resistance that persisted much farther below T_C than LAMH predicted [13], and this was interpreted as direct observation of QPS. A microscopic theory was later developed by Golubev, Zaikin, and co-workers (GZ) [14], and many researchers have since used these ideas to connect their observations to QPS [6, 15, 16].

However, in recent experiments on Pb [17, 18] and MoGe [6, 19, 20] nanowires $\lesssim$ 10 nm wide, the anomalous low-T resistance was *not* observed, and it has been suggested that the earlier observations may have in fact been due to granularity [17, 21] and/or inhomogeneity [22] rather than QPS. Even more striking was the apparent *complete destruction* of superconductivity even as $T \rightarrow 0$ in some of these nanowires with a normal-state resistance $R_n \gtrsim R_Q \equiv h/4e^2$ [6, 18, 20, 23]. Although theories exist for insulating [24–26] or metallic [14, 27, 28] states in 1D as $T \rightarrow 0$, it remains unclear whether any can explain a critical point at $R_n \sim R_Q$. Thus, in spite of extensive theoretical and experimental effort, a complete understanding of QPS has remained elusive.

Then, in 2006, Mooij and Nazarov (MN) [29] conjectured that a symmetry exists between QPS and Josephson tunneling known as *flux-charge duality* [30, 31]. This hypothesis generates a phenomenology of QPS which is dual to that of JJs, including a parallel class of circuits involving 1D superconducting nanowires, what MN called "phase-slip junctions" (PSJs) [29, 32, 33]. Very recently, in fact, two of these circuits have been demonstrated [34, 35], providing the most direct evidence yet seen for QPS. However, MN did not attempt to address the nature or magnitude of QPS, or explain earlier experimental results.

In this work, we describe a new theory built on the hypothesis that QPS and Josephson tunneling are connected by flux-charge duality *at the microscopic level*. Our theory provides a unified, quantitative description of LAMH [10] and Giordano-type [13, 15, 16] fluctuations near T_C, as well as the recent, direct measurements of QPS for $T \rightarrow 0$ [34, 35]. It also suggests an explanation for the observed destruction of superconductivity when $R_n \gtrsim R_Q$ [20], in terms of a *disorder*-driven superconductor-insulator transition (SIT), which is closely connected to phenomena observed in quasi-2D superconductors [3–5, 36].

I. FLUX-CHARGE DUALITY AND QUANTUM PHASE SLIP

Flux-charge duality is a classical symmetry of Maxwell's equations. For lumped-element circuits, it

manifests itself in the invariance of the equations of motion under the duality transformation of fig. 1(a). In continuous media, it can be expressed in terms of the "quasicharge" Q_Σ (defined for a surface Σ) and "fluxoid" Φ_Γ (defined for a curve Γ) [37]:

$$Q_\Sigma = \int_\Sigma dt(\mathbf{J}_Q \cdot \mathbf{da}), \qquad \mathbf{J}_Q = \mathbf{J} + \frac{d\mathbf{D}}{dt} \qquad (1)$$

$$\Phi_\Gamma = \oint_\Gamma dt(\mathbf{E} \cdot \mathbf{ds}), \qquad \mathbf{E} = -\nabla V - \frac{d\mathbf{A}}{dt} \qquad (2)$$

Figures 1(b) and (c) expand on this duality, and show how equations 1 and 2 can both be interpreted as a sum of contributions from "free" and "bound" quasicharge and fluxoid current densities $\mathbf{J}_Q$ and $\mathbf{J}_\Phi$:

$$\mathbf{J}_Q \equiv \underbrace{\rho_Q \mathbf{v}_Q}_{\mathbf{J}_Q^f} + \underbrace{\frac{d\mathbf{D}}{dt}}_{\mathbf{J}_Q^b} \qquad (3)$$

$$\mathbf{J}_\Phi = \mathbf{E} \equiv \underbrace{\mathbf{v}_\Phi \times \mathbf{B}_f}_{\mathbf{J}_\Phi^f} - \underbrace{\frac{d\mathbf{A}}{dt}}_{\mathbf{J}_\Phi^b} \qquad (4)$$

where ρ_Q and $\mathbf{B}_f$ are the free charge and flux densities, and $\mathbf{v}_Q$ and $\mathbf{v}_\Phi$ their velocities. Using the London gauge $\mathbf{A} = -\Lambda \mathbf{J}_Q^f$ for a superconductor (where the kinetic inductivity is $\Lambda = \mu_0 \lambda^2$ with λ the magnetic penetration depth) and $\mathbf{D} = \epsilon \mathbf{E}$ for an insulator, yields:

$$\text{superconductor:} \quad \Lambda \frac{d\mathbf{J}_Q^f}{dt} = \mathbf{J}_\Phi^b \qquad (5)$$

$$\updownarrow$$

$$\text{insulator:} \quad \epsilon \frac{\mathbf{J}_\Phi^f}{dt} = \mathbf{J}_Q^b \qquad (6)$$

In a superconductor, free charge moves ballistically according to eq. 5, which is London's first equation; in an insulator, free fluxoid can be viewed as moving ballistically according to eq. 6, Maxwell's equation for the displacement current. Thus we see that superconductors and insulators are dual.

We now arrive at the duality between a JJ and a PSJ, shown in fig. 2. The former consists of two superconducting islands of Cooper pairs separated by an insulating potential barrier, and the latter, two insulating "islands" of fluxoid quanta (henceforth referred to as "fluxons") separated by a superconducting potential barrier. If we place the surface Σ inside the insulating barrier of a JJ [Fig. 2(e)] with junction capacitance C_J, and the curve Γ inside a superconducting nanowire [Fig. 2(f)] of kinetic inductance L_k (we neglect the geometric inductance), we have:
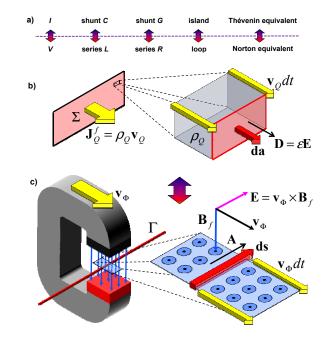

FIG. 1: Flux-charge duality. (a) duality transformation for lumped-element circuits; (b) and (c) the continuous case. (b) The free current density $\mathbf{J}_Q^f = \rho_Q \mathbf{v}_Q$ is the motion of free charge density ρ_Q at a velocity $\mathbf{v}_Q$, through a surface Σ. The bound current density $\mathbf{J}_Q^b = d\mathbf{D}/dt$ is the displacement current density on Σ. (c) An illustrative example of "free" flux density $\mathbf{B}_f$, using a permanent magnet moving at velocity $\mathbf{v}_\Phi$ relative to the stationary curve Γ, with $\mathbf{J}_\Phi^f = \mathbf{v}_\Phi \times \mathbf{B_f}$. In this construction, $\mathbf{J}_\Phi^f \cdot \mathbf{ds}$ is precisely the flux per unit time passing through a segment $\mathbf{ds}$. The bound fluxoid current density $\mathbf{J}_\Phi^b = -d\mathbf{A}/dt$ is associated with time-varying currents flowing along Γ, and the associated voltages from Faraday's law. Although the case of a moving magnet is somewhat artificial, any electric field in a medium can be broken into these two components: $\mathbf{J}_\Phi^f$ associated with fields generated by bound charges, and $\mathbf{J}_\Phi^b$ associated with induced emfs from time varying currents (free charges) flowing in the medium.

$$Q_{JJ} \equiv \underbrace{n2e}_{Q^f} + \underbrace{C_J V}_{Q^b} \qquad (7)$$

$$\Phi_{PSJ} \equiv \underbrace{m\Phi_0}_{\Phi^f} + \underbrace{L_k I}_{\Phi^b} \qquad (8)$$

Here, n is the number of Cooper pairs that have passed through the JJ barrier, and $C_J V$ is the charge on the capacitance C_J of the junction. Similarly, $L_k I$ is the total fluxoid stored in the nanowire due to a current I, and m is the number of fluxons that have "passed through" the wire ($\Phi_0 \equiv h/2e$ is the superconducting flux quantum). For thick enough superconducting wires, the only way for m to be nonzero is if some part of the wire was in the normal state at some time, as occurs in an LAMH phase slip over a length of wire $\sim \xi$, the coherence length. These events are dissipative, produce a measurable voltage pulse, and can be associated with passage of a fluxon

through the null in the superconducting order parameter at a localized position and time. By contrast, we take QPS to be coherent fluxon *tunneling* through the entire length of wire such that: (i) the order parameter remains nonzero and uniform in magnitude, such that no dissipation occurs, and no information about where the phase-slip occurred exists; and (ii) all pairs of fluxon states differing by $m = \pm 1$ are coupled coherently [29]. This is the exact dual of Josephson tunneling.

We now seek to calculate the phase-slip energy E_S, which has been identified [29, 38] with the QPS "rate" estimated by Giordano [13], and later calculated by GZ [14]. In more recent theories it appears in the QPS fugacity and is either taken as the GZ result [24, 26, 28] or left as an unknown [25, 42]. It is also the essential input parameter to the theory of MN, which was observed in recent PSJ experiments [34, 35]. Within our flux-charge duality assumption, E_S is the dual of the Josephson energy E_J for a JJ [29], and we exploit this to calculate it.

The Josephson effect can be understood intuitively using a "macroscopic wavefunction" [43] for the Cooper pairs inside the barrier [44], shown as $\psi_Q(x)$ in fig. 2(g). Because of the finite Cooper pair mass (associated with the kinetic inductivity Λ), it is energetically unfavorable for $\psi_Q(x)$ to *suddenly* drop to zero upon entering the insulator (acquiring fourier components with large momenta), since the resulting zero-point kinetic energy would far exceed the potential energy saved by excluding the Cooper pairs from the insulator. Instead, the total energy is minimized by allowing $\psi_Q(x)$ to penetrate virtually into the insulator over a distance κ_Q^{-1}, such that the average kinetic and potential energies are equal.

We hypothesize that QPS can be understood in a dual manner as virtual penetration of *fluxons* into a *superconductor* [fig. 2(h)] due to their quantum zero-point fluctuations. To illustrate the nature of these fluctuations, we can use the example of fig. 1(c), for which we can write the electrostatic energy density as a kinetic energy density for the moving flux:

$$U_v = \frac{\epsilon |\mathbf{E}|^2}{2} \equiv \frac{\mathcal{P}^2}{2\rho_\Phi} \tag{9}$$

where $\mathcal{P} = \epsilon \mathbf{E} \times \mathbf{B}$ is the electromagnetic momentum density, $\mathbf{E} = \mathbf{v}_\Phi \times \mathbf{B}_f$ (in this example $\mathbf{J}_\Phi^b = \mathbf{0}$), and $\rho_\Phi \equiv \epsilon |\mathbf{B}|^2$ is an effective mass density. Based on this idea, and the identification of moving flux with time-varying Φ [fig. 1(c)], we identify the zero-point fluctuations responsible for QPS with an effective "mass" associated with the permittivity ϵ (dual to the kinetic inductivity Λ). If the fluxon density were to vanish *suddenly* upon entering the superconductor (corresponding to a well-defined phase already *just inside* its surface), this would require fourier components of a *fluxon* wavefunction with large momenta and a large zero-point kinetic energy cost. Just as with Cooper pairs in a JJ, the total energy is reduced when the fluxons (phase fluctuations)
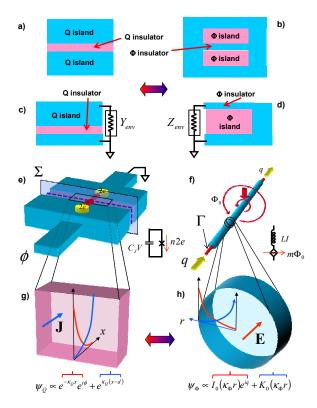

FIG. 2: Microscopic flux-charge duality and quantum phase slip. (a) and (b) show the duality between an isolated JJ and an isolated PSJ (a superconducting nanowire "connecting" two loops); superconductor is shown in blue, insulator in red. The number of Cooper pairs on the islands in (a) and fluxoid quanta in the loops (fluxoid "islands") in (b) are quantized. In (c) and (d) we add an electromagnetic environment, in terms of an admittance Y_{env} or an impedance Z_{env}, with which one of the islands can exchange quanta. This results effectively in a single island coupled via a tunnel barrier to a reservoir. When $Y_{env} \to 0$ (c) becomes an ideal charge qubit and when $Z_{env} \to 0$ (d) becomes an ideal phase-slip qubit [38, 39]. In (e), a JJ is shown with the surface Σ inside the barrier. In this case $Q = C_J V + n(2e)$ where n is the number of Cooper pairs that have tunneled through the barrier; in (f) a PSJ is shown with Γ inside the wire, such that $\Phi = L_k I + m\Phi_0$ where m is the number of fluxoid quanta ("fluxons") that have tunneled through the wire. Note that fluxons are one-dimensional objects [40], shown *for illustrative purposes only* as rings. (g) Illustration of the macroscopic wavefunction ψ_Q for Cooper pairs inside the JJ barrier of thickness d, which can be understood as a superposition of two amplitudes: one with phase ϕ penetrating inward in the $+x$ direction (shown in red), and one with zero phase penetrating inward in the $-x$ direction (blue). (h) The macroscopic wavefunction ψ_Φ for fluxons inside the superconducting wire of radius R, which is a superposition of an amplitude with quasicharge $q = Q/\bar{Q}_0$ penetrating inward in the $-r$ direction (shown in red), and an amplitude with quasicharge zero penetrating outward in the $+r$ direction (blue). These amplitudes are written in terms of the modified Bessel functions K_0, I_0. The effective mass of the Cooper pairs is associated with the kinetic inductivity Λ, which must be "charged up" for them to move. The effective mass of the fluxons is associated with the real part of the permittivity ϵ inside the superconductor, which must be charged up for fluxoid to "move through" (for the phase to fluctuate).

penetrate virtually into the superconductor over a length κ_Φ^{-1}.

This penetration is shown by the macroscopic (fluxon) wavefunction $\psi_\Phi(r)$ in fig. 2(h), which satisfies the Schrödinger-like equation:

$$\left[\frac{\hat{Q}^2}{2\epsilon A} + U_C A \right] \psi_\Phi(r) = 0, \quad r \leq R \quad (10)$$

where $A = \pi R^2$ is the cross-sectional area of the wire, U_C is the condensation energy per volume of the superconductor, and we take $\hat{Q} = -i\bar{Q}_0 R \partial_r$ (with the reduced charge quantum $\bar{Q}_0 \equiv 2e/2\pi$), which is dual to the fluxoid operator for a JJ barrier of thickness d: $\hat{\Phi} = -i\bar{\Phi}_0 d\partial_a$ (with the reduced flux quantum $\bar{\Phi}_0 \equiv \Phi_0/2\pi$). The electric field can now be obtained from the 1D fluxon probability current density associated with the 2D wavefunction $u(r) \equiv \sqrt{r}\psi_\Phi(r)$, thus [45]:

$$E = J_\Phi^f = \frac{\bar{Q}_0}{\epsilon A} \frac{R\,\mathrm{Im}\left[u^\star(r)\partial_r u(r) \right]}{2\pi |u(R)|^2} = E_C \sin q \quad (11)$$

where $q \equiv Q/\bar{Q}_0$, and E_C is the critical electric field, dual to the critical current density J_C for a JJ. The equality on the right is assumed to hold independent of the wire's cross-sectional shape (based on duality [29]), but in the present case it can also be deduced directly from $\psi_\Phi(r)$ in fig. 2(h). The phase-slip energy $E_S = \bar{Q}_0 E_C l$ for a wire of length l can now be written:

$$E_S \approx l\bar{Q}_0 \sqrt{\frac{2U_C}{\epsilon}} \exp\left[-\frac{2A}{\bar{Q}_0}\sqrt{2U_C\epsilon} \right] \quad (12)$$

where the approximate equality holds when the exponent, often called the QPS action [14, 24, 39], is large [45]. Equation 12 indicates that materials with low U_C and ϵ are desirable for strong QPS, and is closely connected to results for 1D JJ arrays [39, 41, 45, 47]. It also provides an intuitive explanation for the kinetic capacitance $C_{k0} \equiv \bar{Q}_0/E_C l$ discussed by MN [29], which is dual to Josephson inductance. To see this, we write it as a permittivity $\epsilon_{k0} \equiv C_{k0} l/A$:

$$\epsilon_{k0} \approx \epsilon \left(\frac{e^{2\kappa_\Phi R}}{\kappa_\Phi R} \right) \quad \kappa_\Phi R \gg 1 \quad (13)$$

This suggests that kinetic capacitance arises directly from the usual permittivity ϵ inside the wire, magnified by a larger effective fluxon mass associated with tunneling through the potential barrier (the factor in parentheses). Although we do not treat the $U_C \to 0$ ($\kappa_\Phi R \to 0$) limit here, we expect that in this limit $\epsilon_k \to \epsilon$ and the fluxons see a simple dielectric rod.
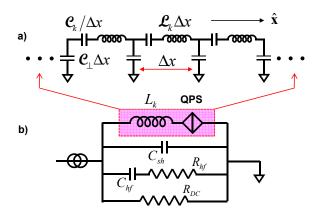

FIG. 3: Model of a PSJ and its electromagnetic environment. We treat the distributed 1D system as a transmission line, where in addition to the usual series (kinetic) inductance $\mathcal{L}_k \Delta x$ and shunt capacitance $\mathcal{C}_\perp \Delta x$ per length Δx, we add a QPS amplitude that can be viewed as a (nonlinear) *series* kinetic capacitance $\mathcal{C}_k/\Delta x = \mathcal{C}_{k0}/\Delta x \sin q$, with $\mathcal{C}_{k0} \equiv \bar{Q}_0/E_C$ (in units of Farads×length) and potential energy $(\bar{Q}_0^2/\mathcal{C}_{k0})\Delta x \cos q$ [29]. This model is the exact dual of a long Josephson junction, with $\mathcal{C}_k$ dual to the Josephson inductance (Henry×length) and the polarization charge on $\mathcal{C}_\perp$ dual to magnetic flux through the geometric inductance of the JJ barrier [45]. (b) Electromagnetic environment model, following [46]. The PSJ is indicated with the notation of ref. [29] (shaded box) with a kinetic inductor L_k in series with a QPS element, described by (lumped-element) energies $E_L \equiv \Phi_0^2/2L_k$ and E_S (dual to $E_C = (2e)^2/2C_J$ and E_J for a JJ). The shunt capacitance C_{sh} is associated with on-chip connections to the sample, R_{DC} with an external current source, and R_{hf} with the high-frequency characteristic impedance looking out of the package in which the sample is mounted. In typical experiments, we have: $R_{DC} \gg R_Q \gg R_{hf}$. We assume also that $\omega_p R_{hf} C_{hf} \gg 1$ such that $Z_{env}(\omega_p) \approx R_{hf} \ll R_Q$.

II. DISTRIBUTED QUANTUM PHASE SLIP JUNCTIONS

The phase slip energy E_S [eq. 12] can be associated with a "bare" quantum phase slip element, in the same manner that the Josephson coupling energy E_J for a JJ includes only the bare Josephson coupling and not yet the effects of the junction barrier capacitance or its geometric inductance (associated with magnetic fields produced inside the junction by currents flowing through it). The dual quantities for a distributed nanowire are its series kinetic inductance per length $\mathcal{L}_k$ and geometric shunt capacitance per length to ground $\mathcal{C}_\perp$, respectively. We incorporate these into a transmission line model, shown in fig. 3(a), in which QPS for a length Δx is shown as a nonlinear series kinetic capacitance $\mathcal{C}_k/\Delta x = \mathcal{C}_{k0}/\Delta x \sin q$, with $\mathcal{C}_{k0} \equiv \bar{Q}_0/E_C$. Note that in calculating E_S and $\mathcal{C}_k$ above, we included only the effect of *bound* charges Q^b (the real part of the permittivity), which describes the dielectric energy cost of the electric fields generated by phase fluctuations. By adding a kinetic inductance $\mathcal{L}_k \Delta x$

in series with each "bare" phase slip element $\mathcal{C}_k/\Delta x$ in fig. 3(a), we have now included free charge Q^f (the imaginary part of the permittivity) as well.

We can now describe fluctuations of the system shown in fig. 3 using the partition function [14, 24]:

$$\mathcal{Z} = \int \mathcal{D}\Psi \exp[-\mathcal{S}(\Psi)/\hbar] \qquad (14)$$

where in the continuum limit $\Delta x \to 0$ the Euclidean (imaginary-time) action is:

$$\mathcal{S} = \int_0^{\hbar\beta} d\tau \int dx \left\{ \frac{\mathcal{C}_\perp V^2}{2} + \frac{\mathcal{L}_k I^2}{2} + \frac{\bar{Q}_0^2}{\mathcal{C}_{k0}} \cos q \right\} \quad (15)$$

and $\beta \equiv 1/k_B T$, $\tau \equiv it$. The functional integral in eq. 14 is carried out over paths Ψ in x, τ which begin (at $\tau = 0$) and end (at $\tau = \hbar\beta$) in the uniform superconducting state (about which we consider fluctuations). We assume that Gaussian fluctuations can be factorized out in eq. 14 (such that they simply renormalize the bare parameter values in $\mathcal{S}$ [24]), leaving only topologically nontrivial paths to be evaluated.

To identify these paths, we note that the Wick rotation $t \to -i\tau$ inherent in eq. 15 can be viewed as a transformation of a 1+1D classical dynamics problem into a 2D statics problem, and define:

$$\mathbf{y} \equiv c_s \tau \hat{\mathbf{t}} \qquad (16)$$

where $c_s \equiv \sqrt{1/\mathcal{L}_k \mathcal{C}_\perp}$ is the Mooij-Schön velocity [48]. We then obtain the following 2D equation of "motion":

$$\lambda_E^2 \nabla_{xy}^2 q + \sin q = 0 \qquad (17)$$

where $\nabla_{xy} = \hat{\mathbf{x}}\partial_x + \hat{\mathbf{y}}\partial_y$, we have used $I/c_s = \bar{Q}_0 \partial_y q$ and $\mathcal{C}_\perp V = -\bar{Q}_0 \partial_x q$, and defined an *electric* penetration length:

$$\lambda_E \equiv \sqrt{\frac{\bar{Q}_0}{E_C \mathcal{C}_\perp}} \equiv \frac{c_s}{\omega_p} = \sqrt{\frac{\mathcal{C}_{k0}}{\mathcal{C}_\perp}} \qquad (18)$$

and QPS plasma frequency $\omega_p \equiv \sqrt{1/\mathcal{L}_k \mathcal{C}_{k0}}$, which are dual to the Josephson penetration depth and plasma frequency [29]. After some manipulations, we can describe fig. 3(a) thus:

$$Z_L \nabla_{xy} \times \mathbf{d} = \mathbf{j} \qquad (19)$$

$$\nabla_{xy} \times \mathbf{j} = -\frac{\mathbf{E}}{c_s} \qquad (20)$$

with $Z_L \equiv \sqrt{\mathcal{L}_k/\mathcal{C}_\perp}$ the linear impedance of the line, and the definitions:

$$\mathbf{E} \equiv E\hat{\mathbf{z}}$$
$$\mathbf{d} \equiv Q\hat{\mathbf{z}} \equiv \epsilon_k A\mathbf{E}$$
$$\mathbf{j} \equiv \nabla_{xy}\Phi = \mathcal{L}_k I\hat{\mathbf{x}} + Z_L \rho_\perp \hat{\mathbf{y}} \qquad (21)$$

Here, $\rho_\perp = \mathcal{C}_\perp V$ is the charge per length on $\mathcal{C}_\perp$, and continuity requires that $\nabla_{xy} \cdot \mathbf{j} = 0$ [fig. 3(a)] (note that the $\hat{\mathbf{z}}$ direction is *fictitious* here, and is only introduced to use the curl notation in eqs. 19,20). Equations 19 and 20 are identical in form to Ampère's law and London's second equation, in 2D, which govern the penetration of magnetic flux oriented along $\hat{\mathbf{z}}$ into a superconductor [43]; however, these equations govern the penetration of *electric field* into a superconducting wire in 1+1D. In fact, it turns out that nearly all of the well-known magnetic results in 2D have analogs here, including an *electric* Meissner effect, and type I and type II *electric* flux penetration [45].

We focus on the (electric) type II limit where $\lambda_E \gg \xi$, which in most cases is appropriate for $T \to 0$ (where U_C is largest and ξ is smallest). We seek an *electric* vortex solution to eqs. 19-21, in which a normal core of size $\sim \xi$ in x, y is surrounded by circulating screening currents $\mathbf{j}$ [eq. 21] extending out to $\sim \lambda_E$. In order to include only closed paths in eqs. 14 and 15, we impose the condition (analogous to fluxoid quantization in 2D):

$$\oint_\sigma \mathbf{j} \cdot \mathbf{ds} + \int_\alpha \frac{\mathbf{E}}{c_s} \cdot \mathbf{da} = \pm\Phi_0 \qquad (22)$$

where σ is a closed curve in the xy plane which contains the core and bounds the surface α [fig. 4(a)]. This condition means that the fluxoid evolves by Φ_0 ($-\Phi_0$) over the course of the event, which we call a "type II phase slip" (anti-phase slip). Using eqs. 19-22, and assuming $\epsilon_k \approx \epsilon_{k0}$ far from the core (analogous to $\Lambda(J) \approx \Lambda(0)$ for a magnetic vortex [43]), we obtain [fig. 4]:

$$\mathbf{j}(\rho) \approx \pm\frac{\bar{\Phi}_0}{\lambda_E} K_1\left(\frac{\rho}{\lambda_E}\right)\hat{\phi}, \ \ \rho \gg \xi \qquad (23)$$

where K is the modified Bessel function, $\rho \equiv \sqrt{x^2 + y^2}$, and we assume $\hbar\beta \gg \lambda_E/c_s = \omega_p^{-1}$. We can also deduce an interaction between type II phase slips separated by $\delta\rho \equiv |\vec{\rho}_1 - \vec{\rho}_2|$:

$$\frac{\mathcal{S}_{int}(\delta\rho)}{\hbar} \approx \pm\frac{R_Q}{Z_L} K_0\left(\frac{\delta\rho}{\lambda_E}\right), \ \ \delta\rho \gg \xi \qquad (24)$$

where the sign is negative for a phase slip-anti phase slip pair. Both of these results are analogous to their magnetic vortex counterparts [43], and this can be exploited to understand their implications.
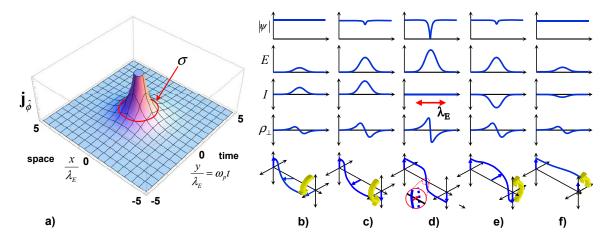
FIG. 4: Type II phase slip in a 1D superconductor. In 1+1D, a normal core of size ξ is surrounded by circulating "currents" $\mathbf{j}$ [eqs. 21, 23] plotted in (a). A possible curve σ for the line integral of eq. 22 is shown in red. Panels (b)-(f) show the order parameter along the wire as a phasor, at different times. On the leading edge of the vortex, current begins to flow over a length $\sim \lambda_E$ in the $+\hat{\mathbf{x}}$ direction (b); this begins to charge up $\mathcal{C}_k$, producing a gradient in $j_y = Z_L \rho_\perp$. Once the total fluxoid across the wire comes close to $\Phi_0/2$ (c), the order parameter can evolve continuously to a state (d) in which the current is zero and there is a null at the center of the vortex of length $\sim \xi$. This is the core of the type II phase slip and is closely related to the well-known saddle-point solution encountered in long weak links [51] and for LAMH phase slips [7, 8]. At this point the order parameter "passes through" the x-axis, and the supercurrent reverses (e). The current in the $-\hat{\mathbf{x}}$ direction then discharges the kinetic capacitance as it ramps down to zero (f). This "static" solution in our x, y coordinates corresponds to an instanton-like solution [14, 24, 47] in x, t. We emphasize that this is a *quasi-classical* solution for fluxoid evolution by $\pm\Phi_0$, which is conceptually distinct from QPS in the same way that Bloch oscillation in a JJ [31] is distinct from Josephson tunneling.

III. COMPARISON WITH EXPERIMENTS

Before connecting our work to experiments, we must first include the effect of the electromagnetic environment. Our model is shown in fig. 3(b), whose most important feature is a low, resistive impedance $R_{hf} \lesssim \sqrt{\mu_0/\epsilon_0}$ at the phase slip plasma frequency ω_p (In the cases of interest here, ω_p will be sufficiently high that this is a resonable assumption unless special precautions are taken [35, 52]). With $R_{hf} \ll R_Q$, gaussian phase fluctuations at ω_p are strongly damped; if also $R_{hf} \ll Z_L$, the classical boundary condition at the wire ends is approximately just a short, and can be applied using the method of images [24]. The resulting current distribution for a type II phase slip when $l < \lambda_E$ is shown in Fig. 5(a) (image phase slips are shown with dashed lines), which can be viewed as the adiabatic evolution along one period of the lowest energy band $U_0(\Phi)$ in fig. 5(c) (dashed arrow) [25]; in JJ language, the "phase particle" (whose "position" is Φ) jumps from one "potential well" of the lowest band $U_0(\Phi)$ to the next [46]. This process can only occur, however, if phase fluctuations of the environment can excite the system over the barrier. Thus, we see that QPS is masked by a low $R_{env}(\omega_p) \ll R_Q$ [24], where for low currents $U_0(\Phi) \approx \Phi^2/2L_k$ - the wire looks like a uniform superconductor.

The effect of an external bias current I_b can be described, just as for JJs, by an additional potential energy:

$$U_n(I_b, \Phi) = U_n(\Phi) - I_b\Phi \qquad (25)$$

which lowers the potential barrier for phase slips in one direction while raising it in the other [6, 8, 45] [fig. 5(e),(f)]. As the barrier is lowered by increasing I_b, the phase particle has an increasing chance to surmount it per unit time due to a (thermal or quantum) phase fluctuation. If this occurs, it can either be re-trapped in the adjacent potential well by the damping due to R_{hf}, or it can "escape" into the voltage state corresponding to a terminal velocity $V = \dot{\Phi}$ (determined by its effective mass and the damping). This is the "deconfinement" of ref. [24]. In the experiments of ref. [19], escape rates were measured vs. I_b and these data were fitted to determine an "effective temperature" T_{eff} for the phase fluctuations [11]. At higher T, it was found that $T \approx T_{eff}$, while at low temperatures T_{eff} saturated at a minimum value T_Q, and this was taken as a signature of QPS [19] (this is very similar to the method used to observe macroscopic quantum tunneling in JJs [11]). In our model, however, we expect an apparent T_Q which is not directly associated with QPS, but rather with the quantum fluctuations of the damped oscillator formed by C_{sh}, L_k, and R_{hf} [fig. 3(b)] [53]. Figure 5(g) shows that this expectation is indeed consistent with the observations in ref. [19] for four of the five reported wires. We can also compare the average switching current I_{sw} observed in ref. [19] with our prediction based on eq. 25. Figure. 5(h) shows that the agreement is also very good for the same four wires.
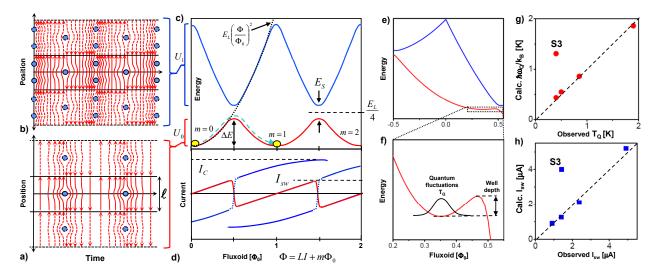
FIG. 5: Type II phase-slip in a low-impedance environment. (a) and (b) show the two lowest-energy Type II phase slip "lattices" for a constant voltage $V = \dot{\Phi}$ across a short wire ($l \lesssim \lambda_E$), when $R_{env}(\omega_p) \ll R_Q$, Z_L (These are analogous to Abrikosov lattices of magnetic vortices in superconducting strips of finite width). Image phase slips are shown with dashed lines, and result in currents that are nearly uniform along the wire, except near the cores of the type II phase slips (blue circles). (c) two lowest PSJ energy bands $U_0(\Phi)$ and $U_1(\Phi)$ (which are exactly dual to the quasicharge bands of a JJ in a high-Z environment [31]). Inductive parabolae with $E = E_L(\Phi/\Phi_0 - m)^2$ are degenerate at $E = E_L/4$, where an avoided crossing occurs due to E_S [29, 38, 39]. If $E_S \to 0$, the wire is simply an inductance L_k with energy $E_L(\Phi/\Phi_0^2)$ (dashed black line). The current distribution shown in (a) for a short wire corresponds to adiabatic evolution along the lowest band shown by the dashed arrow in (c), which is dual to Bloch oscillation of a JJ [31]. If the traversal remains adiabatic, the dynamics are insensitive to the magnitude of E_S. Note that ΔE is smaller than the LAMH barrier by a factor of $\sim \xi/l$, due to work done by the source [45], and for $E_S \ll E_L$ is essentially the energy to charge up L_k with $\Phi = \Phi_0/2$ [55]. (d) shows the current-phase relation for the nanowire, which is nearly the same as for a long superconducting weak link [51], but with additional avoided crossings associated with QPS, which produce a switching current $I_{sw} < I_C$ into a voltage state. (e) lowest two calculated energy bands $U_0(I_b, \Phi)$ and $U_1(I_b, \Phi)$ for wire S1 of ref. [19] at $I_b = 2$ μA [45]. (f) expanded view of the residual potential well in $U_0(I_b, \Phi)$. Fluctuations of the $L_k - R_{hf} - C_{sh}$ circuit produced by the wire and its environment can cause the phase particle to escape from this well even when there is still a potential barrier, at which point a voltage appears [11, 46]. (g) calculated quantum temperature T_Q [45] for wires S1-5 of ref. [19] (based on ref. [53]) vs. the observed T_Q at $T = 0.3K$ [19]. With the exception of wire S3, the agreement is excellent, where the free parameters were (i) $R_{env}(\omega_p)$, for which the linear fit gives 115Ω, and (ii) C_{sh}, to which the results are insensitive as long as the system is overdamped ($R_{hf}C_{sh} < \sqrt{L_kC_{sh}}$), which is true here for $C_{sh} \lesssim 10$ fF. (h) Solid symbols are calculated values [45] of I_{sw} plotted vs. the observed switching currents [54] for wires S1-5 in ref. [19]. The predictions are derived from eq. 25, assuming that switching occurs when the potential well depth is equal to the observed T_Q [45]. Two adjustable parameters were used (i) a constant a used to determine L_k from R_n according to: $L_k = a\hbar R_n/k_B T_C$ [38]; and (ii) ϵ. With $a = 0.21$ and $\epsilon = 25\epsilon_0$, we find good agreement except again for wire S3. An estimate of $a = 0.14$ appears in ref. [38] and ϵ is not known.

Our model also suggests a different explanation for another observation in ref. [19] that was was highlighted as direct evidence for QPS: the fact that the width of the stochastic probability distributions $P(I_{sw})$ (obtained from many repeated I_{sw} measurements) increased as T was lowered. Since the system is overdamped, at high T the phase particle moving in the potential $U_0(I_b, \Phi)$ can be thermally excited over a barrier many times (undergo many phase slips), each time being re-trapped by the damping, before it happens to escape into the voltage state. At low T, these excitations are sufficiently rare that in a given time it is more likely to experience a single fluctuation strong enough to cause escape than it is to experience multiple weaker fluctuations which act together to cause escape. Just as for JJs, this produces a $P(I_{sw})$ that broadens as T is lowered [46], since fewer phase slips are associated with each switching event, and the result-

ing stochastic fluctuations of I_{sw} are larger. Note that in contrast to ref. [19], where these results were explained by local heating of the wire by individual quantum phase slips, in our model the energy $I_b\Phi_0$ released during a type II phase slip is dissipated in the environment R_{hf}.

So far we have focused on $T \ll T_C$. However, much experimental work has focused on the region near T_C where the condensation energy U_C goes to zero. In this regime, it turns out that the ratio λ_E/ξ is typically less than unity, corresponding to the type I case for electric flux penetration (this is in contrast to the magnetic case, where the Ginzburg-Landau $\kappa = \lambda/\xi$ is a temperature-independent material property). The corresponding "type I phase slip" consists of a null in the order parameter of dimension ξ, inside which is contained a pulse of E with total area Φ_0. Screening currents $\mathbf{j}$ of dimension $\lambda_E < \xi$ flow around this region of nonzero E
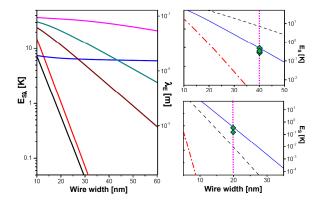
FIG. 6: Quantum phase slip energy. (a) Calculated $E_{S\lambda} = \bar{Q}_0^2/\mathcal{C}_\perp \lambda_E$, which is the phase slip energy E_S for a wire with length $l = \lambda_E$ (plotted on the right axis for $\mathcal{C}_\perp =$50 pF/m) [45]. For a given width, the E_S value on the left axis corresponds to the wire length l on the right axis. With the exception of the MoGe relevant to refs. [15, 19, 20, 23], all of the materials shown are known for their low superfluid density (associated with a low carrier density in the metallic state) [1] which corresponds directly to low U_C and therefore strong QPS. (blue) 12.5 nm thick a-Nb$_{0.15}$Si$_{0.85}$ [56]; (blue) 5 nm TiN [3]; (green) 20 nm a-InO$_x$ [4]; (brown) 35-nm a-InO$_x$ [34]; (black) 10 nm thick a-Nb$_{0.45}$Si$_{0.55}$ [35]. We also show (red) 9 nm Mo$_{0.79}$Ge$_{0.21}$ from ref. [19]. Note that our model assumed $2R < \xi$, and treated the wire as cylindrical. (b) and (c) show E_S vs. wire width for the materials and wire lengths of refs. [34] and [35] (sample A), respectively, with the vertical dashed line indicating the experimental width, and the filled circles the observed values. The dashed black line is the Giordano estimate [13, 15, 19, 38], the red dot-dash line is the prediction of GZ [?], and the solid blue line is our prediction [45].

[45]. These events are in fact none other than LAMH phase slips [7, 8, 10], and in most cases a continuous transition occurs from type I to type II as T is lowered.

This picture suggests a new interpretation of Giordano's original experiments [13], in which LAMH-type behavior near T_C was observed to cross over at lower temperatures to a weaker scaling with $T - T_C$. At low enough T where the type II limit is reached, if $\lambda_E > l$, the energy barrier in our model is $\approx E_L/4$ (for $E_S \ll E_L$) [fig. 5(c)]. This scales as $\propto T - T_C$ (compared to $\propto (T - T_C)^{3/2}$ in the LAMH regime), exactly as observed [45]. We therefore interpret the crossover observed by Giordano *not* as a transition from thermal to quantum fluctuations, but instead as a crossover between different energy barriers for purely thermal fluctuations [55]. Near T_C we have the usual LAMH barrier, but far below T_C this crosses over in the type II limit when $\lambda_E > l$ to an *inductive* energy barrier. This picture can also explain the mysterious fact that Giordano's anomalous low-T resistance was *not* observed in refs. [19, 20], even though the wires had cross-sectional areas nearly 50 times smaller (which is difficult to explain in any theory where the low-T resistance is directly identified with QPS). For the wires of ref. [19], our calculated E_S is so large that λ_E stays

comparable to ξ, and never becomes longer than l, even as $T \to 0$. Therefore, LAMH-type scaling is expected at all temperatures even though the QPS itself is much stronger.

Our discussion has revealed that in a low-Z environment, even at $T = 0$, QPS can be observed in transport measurements only indirectly. As long as the avoided crossings in fig. 5(c) are large enough to suppress Landau-Zener transitions, the magnitude of E_S has little if an effect on the result. However, E_S is perhaps the quantity of greatest interest, both fundamentally and for possible devices. Figure 6(a) shows this quantity calculated for several materials, with the wire length l set equal to λ_E. We find that E_S can in fact be quite large for reasonable wire dimensions. This might appear counterintuitive given the apparent difficulty of observing it, but in fact we claim this difficulty has been a consequence only of the low-Z environments (at ω_p) used in nearly all experiments.

Very recently, however, two experimental groups have attempted to circumvent this problem, and appear to have observed E_S directly. In the first, using a-InO films, Astafiev and co-workers demonstrated the phase-slip qubit of ref. [38], in which the nanowire forms a closed loop. Although this can be viewed as $Z_{env} = 0$, the fixed phase boundary condition imposed by flux threading a closed superconducting loop allows the PSJ to be biased exactly on the avoided crossing of width E_S shown in fig. 25. In this case direct spectroscopic measurement yielded $E_S/h \sim$ 5-10 GHz [34]. The second experiment used a-Nb$_{0.45}$Si$_{0.55}$ nanowires embedded in an environment formed by highly-resistive Cr nanowires. Although the parasitic reactance of these wires likely reduces the impedance at high frequencies [46], the authors were able to observe the Coulomb blockade associated with $V_C \sim 20 - 100\mu$V [35]. Figures 6(b) and (c) show a comparison of our predictions with these results, in both cases showing reasonable agreement. For comparison we also show the predictions of Giordano's model [13, 15, 19, 38], and that of GZ [14], which are significantly different from both observations.

IV. DESTRUCTION OF SUPERCONDUCTIVITY IN 1D

We now turn to the destruction of superconductivity down to $T = 0$ for short wires with $R_n \gtrsim R_Q$. Previous theories have predicted insulating or metallic behavior as the wire diameter [14], the characteristic impedance Z_L [14, 24], or an external shunt resistor [24] is tuned through a critical value, under various conditions. However, none can obviously explain a $T = 0$ transition at $R_n \sim R_Q$. In all of these theories the predicted transition relies on the presence of a form of dissipation which somehow remains even as $T \to 0$, such as anomalous excited quasiparticles [28], a resistive shunt [24], continuum plasmon modes [14, 24], or the quantum phase-slips themselves [26].

We propose an alternative view, in which a $T = 0$ SIT is driven by *disorder*-induced phase fluctuations. This is analogous to the SIT observed in some quasi-2D systems with low superfluid density [3, 4] when the sheet resistance $R_\square \gtrsim R_Q$ [49]. This 2D disorder-induced SIT has been interpreted using the "dirty boson" model of Fisher and co-workers [5], in which disorder nucleates (virtual) unbound vortex-antivortex pairs (VAPs), with sufficient strength that these unpaired vortices themselves form a Bose-condensate, destroying long-range phase coherence and producing a gapped insulator [5]. This is closely related to the Berezinskii-Kosterlitz-Thouless (BKT) vortex-unbinding transition in the classical 2D XY model [50].

To connect these ideas to our system, we recall that the imaginary-time path-integral of eq. 14 represents an isomorphism between closed Feynman paths describing the quantum ground state of a 1D system at $T = 0$ and statistical configurations of a *classical* 2D system at finite T [47, 59]. This mapping has been exploited to predict in 1D a $T = 0$ quantum analog of the classical BKT transition [14, 24, 47], a phenomenon known as *instanton condensation* [47, 59] (referred to as "proliferation" of phase slips in refs. [14, 24, 25, 55]). We can apply this idea directly to our type II phase-slips: as the disorder is increased, amplitudes for broken phase slip-anti phase slip pairs (closed paths in eq. 15) increase in the ground state, until at some critical point they overlap sufficiently to form a condensate. In the dirty boson model, the $T = 0$ critical point at $R_\square \sim R_Q = \Phi_0/(2e)^2$ corresponds to approximately one vortex crossing for every Cooper pair crossing [5]. In our 1D case, the corresponding critical point would appear to be $R_n \sim R_Q$. In fact, in a recent experiment using "honeycomb" bismuth films, consisting essentially of a 2D network of nanowires, a SIT was observed precisely when R_n *of each nanowire* passed through R_Q (by tuning the film thickness) [60], supporting our proposed connection between the 1D and 2D phenomena.

This connection may also explain why in longer MoGe nanowires (greater than a few hundred nm), the SIT is no longer observed [6, 15]. As can be seen in Fig. 6(a), our theory predicts $\lambda_E \sim$200-300 nm for MoGe wires 7-10 nm wide. Since the logarithmic interaction required for the BKT-like quantum transition only persists to separations $\rho \sim \lambda_E$ [c.f. eq. 24], we would indeed expect to see a disappearance of the SIT as the wire becomes significantly longer than this [61]. We note that the observed reduction in T_C near the SIT [20, 23], which is not predicted by the dirty boson model, may be explained by the gap suppression observed in 2D for similar MoGe films [58], and believed to be due to an enhanced Coulomb interaction [62, 63].

V. CONCLUSION

We have described a new theory for quantum phase fluctuations in 1D built on the hypothesis that flux-charge duality [29] holds at the microscopic level between these fluctuations and the charge fluctuations associated with Josephson tunneling. While previous theories have treated QPS essentially as a quantum version of LAMH phase slips (having a normal core inside which the order parameter goes to zero [14, 24, 26, 28]), in our theory QPS is a *tunneling* process involving fluctuation *of the phase only*. In a low-impedance environment, quasi-classical phase-slip excitations with a normal core arise out of this theory (in the same manner that Bloch oscillations in JJs arise from Josephson tunneling) which are electric analogs of the penetration of single magnetic flux quanta in 2D. In terms of these excitations, we can provide a quantitative description of nearly all phenomena observed for quasi-1D superconducting wires in low-Z environments, including LAMH phase slips [8, 10], Giordano's "resistive tails" [13], and anomalous IV characteristics of ultranarrow MoGe wires [15, 19, 20, 23]. We also predict values for the phase slip energy E_S is good agreement with recent observations. Finally, our model suggests a mechanism for the observed SIT in short wires when $R_n \gtrsim R_Q$, in terms of a disorder-driven quantum phase transition [5, 36].

An exciting result of our theory is the prediction that it should be feasible to achieve large enough E_S to build dual circuits to *classical* Josephson devices, such as a quantum standard of current [29, 31] dual to the Josephson voltage standard, or sensitive electrometers based on the circuit of ref. [35] (dual to the DC SQUID). Another interesting possibility would be the dual of RSFQ digital circuits: a voltage-state logic in which Cooper pairs are shuttled between islands [45]. It would have no static power dissipation, and could be amenable to integration with charge-based memory elements.

[1] V.J. Emery and S.A. Kivelson, Nature **374**, 434 (1995).

[2] M.A. Steiner, G. Boebinger, and A. Kapitulnik, Phys. Rev. Lett. **94**, 107008 (2005).

[3] T.I. Baturina, A.Y. Mironov, V.M. Vinokur, M.R. Baklanov, and C. Strunk, Phys. Rev. Lett. **99**, 257003 (2007)

[4] G. Sambandamurthy, L.W. Engel, A. Johansson, and D.

Shahar, Phys. Rev. Lett. **92**, 107005 (2004).

[5] M.P.A. Fisher, Phys. Rev. Lett. **65**, 923 (1990).

[6] A. Bezryadin, J. Phys. Condens. Matter **20**, 1 (2008).

[7] W.A. Little, Phys. Rev. **156**, 396 (1967).

[8] J.S. Langer and V. Ambegaokar, Phys. Rev. **164**, 498 (1967); D.E. McCumber and B.I. Halperin, Phys. Rev. B **1**, 1054 (1970).

[9] I.H. Duru, H. Kleinert, N. and Ünal, J. Low Temp. Phys. **42**, 137 (1981).

[10] W.W. Webb, and R.J. Warburton, Phys. Rev. Lett. bf 20, 461 (1968); R.S. Newbower, M.R. Beasley, and M. Tinkham, Phys. Rev. B **5**, 864 (1972).

[11] J.M. Martinis, M.H. Devoret, and J. Clarke, Phys. Rev. B **35**, 4682 (1987)

[12] A.J. van Run, J. Romijn, and J.E. Mooij, Jpn. J. Appl. Phys. Supplement 26-3-2, 1765 (1987).

[13] N. Giordano, Phys. Rev. Lett. **61**, 2137 (1988).

[14] A.D. Zaikin, D.S. Golubev, A. van Otterlo, and G.T. Zimányi, Phys. Rev. Lett. **78**, 1552 (1997); D.S. Golubev and A.D. Zaikin, *Quantum tunneling of the order parameter in superconducting nanowires*, Phys. Rev. B **64**, 014504 (2001).

[15] C.N. Lau, N. Markovic, M. Bockrath, A. Bezryadin, and M. Tinkham, Phys. Rev. Lett. **87**, 217003 (2001)

[16] F. Altomare, A.M. Chang, M.R. Melloch, Y. Hong, and C.W. Tu, Phys. Rev. Lett. **97**, 017001 (2006);M. Zgirski, K.-P. Riikonen, V. Touboltsev, and K.Yu. Arutyunov, Phys. Rev. B **77**, 054508 (2008).

[17] A.V. Herzog, P. Xiong, F. Sharifi, and R.C. Dynes, Phys. Rev. Lett. **76**, 668 (1996).

[18] P. Xiong, A.V. Herzog, and R.C. Dynes, Phys. Rev. Lett. **78**, 927 (1997).

[19] M. Sahu, M.-H. Bae, A. Rogachev, D. Pekker, T.-C. Wei, N. Shah, P.M. Goldbart, and A. Bezryadin, Nature Physics **5**, 506 (2009).

[20] A.T. Bollinger, R.C. Dinsmore, A. Rogachev, and A. Bezryadin, Phys. Rev. Lett. **101**, 227003 (2008).

[21] J.-M. Duan, Phys. Rev. Lett. **74**, 5128 (1995).

[22] M. Zgirski and K.Yu. Arutyunov, Phys. Rev. B **75**, 172509 (2007).

[23] A. Bezryadin, C.N. Lau, and M. Tinkham, Nature **404** 971 (2000).

[24] H.P. Büchler, V.B. Geshkenbein, and G. Blatter, Phys. Rev. Lett. **92**, 067007 (2004).

[25] S. Khlebnikov and L.P. Pryadko, Phys. Rev. Lett. **95**, 107007 (2005).

[26] D. Meidan, Y. Oreg, and G. Refael, Phys. Rev. Lett. **98**, 187001, (2007).

[27] S. Sachdev, P. Werner, and M. Troyer, Phys. Rev. Lett. **92**, 237003 (2004).

[28] G. Refael, E. Demler, and Y. Oreg, Phys. Rev. B **79**, 094524 (2009).

[29] J.E. Mooij and Yu.V. Nazarov, Nature Physics **2**, 169 (2006).

[30] A. Davidson and M.R. Beasley, IEEE J. Solid State Circuits, **SC-14** 758 (1979); K.K. Likharev, IEEE Trans. Mag. **23**, 1142 (1987); A.M. Kadin, J. Appl. Phys **68**, 5741 (1990).

[31] W. Guichard and F.W.J. Hekking, Phys. Rev. B **81**, 064508 (2010).

[32] A.M. Hriscu and Yu.V. Nazarov, Phys. Rev. Lett. **106**, 077004 (2011).

[33] A.M. Hriscu and Yu.V. Nazarov, Phys. Rev. B **83**, 174511 (2011).

[34] O. Astafiev, Private communication.

[35] T.T. Hongisto and A.B. Zorin, arXiv:1109.3634.

[36] B. Sacépé, T. Dubouchet, C. Chapelier, M. Sanquier, M. Ovadia, D. Shahar, M. Feigel'man, and L. Ioffe, Nature Physics **7**, 239 (2011).

[37] M.H. Devoret, in "Quantum Fluctuations", Les Houches summer school 1995, eds. S. Reynaud, E. Giacobino, and J. Zinn-Justin.

[38] J.E. Mooij and C.J.P.M. Harmans, N. J. Phys. **7** 219 (2005).

[39] K.A. Matveev, A.I. Larkin, and L.I. Glazman, Phys. Rev. Lett. **89**, 096802 (2002).

[40] D. Rohrlich, J. Phys. A 43, 354028 (2010).

[41] V.E. Manucharyan, N.A. Masluk, A. Kamal, J. Koch, L.I. Glazman, and M.H. Devoret, Phys. Rev. B **85**, 024521 (2012).

[42] S. Khlebnikov, Phys. Rev. B **78**, 014512 (2008).

[43] T.P. Orlando and K.A. Delin, *Foundations of Applied Superconductivity*, Addison-Wesley, 1991.

[44] More precisely, this wavefunction can be identified with Gor'kov's anomalous Green's function [see, e.g., V. Ambegaokar and A. Baratoff, Phys. Rev. Lett. **10**, 486 (1963)].

[45] See supplementary material.

[46] R.L. Kautz and J.M. Martinis, Phys. Rev. B **42**, 9903 (1990).

[47] R.M. Bradley and S. Doniach, Phys. Rev. B **30**, 1138, (1984).

[48] J.E. Mooij and G. Schön, Phys. Rev. Lett. **55**, 114 (1985).

[49] In these materials, evidence for a nonzero gap is observed even in the insulating state [36], indicating that phase fluctuations drive the transition. A similar disorder-driven SIT at $R_\square \sim R_Q$ is also observed in some other materials with higher superfluid density [57, 58] which is believed to result from a different mechanism not associated with phase fluctuations [63].

[50] J.M. Kosterlitz, J. Phys. C **7**, 1046 (1974), and references therein.

[51] K.K. Likharev, Rev. Mod. Phys. **51**, 101 (1979).

[52] S. Corlevi, W. Guichard, F.W.J. Hekking, and D.B. Haviland, Phys. Rev. Lett. **97** 096802 (2006).

[53] H. Grabert and U. Weiss, Phys. Rev. Lett. **53**, 1787 (1984).

[54] A. Bezryadin, private communication.

[55] S. Khlebnikov, Phys. Rev. B **77**, 014505 (2008).

[56] C.A. Marrache-Kikuchi, H. Aubin, A. Pourret, K. Behnia, J. Lesueur, L. Bergé, and L. Dumoulin, Phys. Rev. B **78**, 144520 (2008).

[57] D.B. Haviland, Y. Liu, and A.M. Goldman, Phys. Rev. Lett. **62** 2180 (1989).

[58] J.M. Graybeal and M.R. Beasley, Phys. Rev. B **29**, 4167 (1984).

[59] E. Fradkin and L. Susskind, Phys. Rev. D, 2637 (1978).

[60] M.D. Stewart, Jr., A. Yin, J.M. Xu, and J.M. Valles, Jr., Science **318**, 1273 (2007).

[61] M.R. Beasley, J.E. Mooij, and T.P. Orlando, Phys. Rev. Lett. **42**, 1165 (1979).

[62] Y. Oreg and A.M. Finkel'stein, Phys. Rev. Lett. **83**, 191 (1999).

[63] A.M. Finkel'stein, Physica B **197**, 636 (1994).

Flux-charge duality and quantum phase fluctuations in one-dimensional superconductors: Supplementary material

Andrew J. Kerman

Lincoln Laboratory, Massachusetts Institute of Technology, Lexington, MA, 02420

(Dated: January 26, 2023)

PACS numbers:

I. DETAILS ON THE DERIVATION OF AN EXPRESSION FOR THE ELECTRIC FIELD USING DUALITY

Here we describe the reasoning behind eqs. 10 and 11 in the text which allow us to calculate E_C using the probability flux density for the macroscopic fluxon wavefunction. Following ref. 7, we write zero-energy, time-independent Schrödinger equations for ψ_Q and ψ_Φ. In eq. 1 below, $U_I \equiv U_{cp} n_s$ can be viewed as the potential

energy density for the superconducting state to penetrate into the insulator, and U_C (the condensation energy) as the potential energy density for the insulating state to penetrate into the superconductor. We have also defined the specific inductance and capacitance: $\mathcal{L}_A \equiv \Lambda d$ and $\mathcal{C}_l \equiv \epsilon A$. The former can be viewed as the kinetic inductance $\times$ area for the superconducting state inside the junction barrier, and the latter the capacitance $\times$ length of the insulating state inside the superconductor.

$$\left[\frac{\hat{\Phi}^2}{2\mathcal{L}_A} + U_I d\right]\psi_Q(x) = 0, \quad 0 \le x \le d \quad \Longleftrightarrow \quad \left[\frac{\hat{Q}^2}{2\mathcal{C}_l} + U_C A\right]\psi_\Phi(r) = 0, \quad r \le R \tag{1}$$

$$\hat{\Phi} = -i\bar{\Phi}_0 d\partial_x \quad \Longleftrightarrow \quad \hat{Q} = -i\bar{Q}_0 R\partial_r \tag{2}$$

$$\kappa_Q d = \frac{\sqrt{2d\mathcal{L}_A U_I}}{\bar{\Phi}_0} \quad \Longleftrightarrow \quad \kappa_\Phi R = \frac{\sqrt{2A\mathcal{C}_l U_C}}{\bar{Q}_0} \tag{3}$$

$$J = \frac{\bar{\Phi}_0}{\mathcal{L}_A}\frac{d\,\mathrm{Im}\left[\psi_Q^\star(x)\partial_x\psi_Q(x)\right]}{|\psi_Q(0)|^2} = J_C \sin\phi \quad \Longleftrightarrow \quad E = \frac{\bar{Q}_0}{\mathcal{C}_l}\frac{R\,\mathrm{Im}\left[u^\star(r)\partial_r u(r)\right]}{2\pi|u(R)|^2} = E_C \sin q \tag{4}$$

To solve eqs. 1 we use the fluxoid and quasicharge operators of eq. 2. For the JJ case, using the semiclassical result $\Lambda = 2m/(2e)^2 n_s$ [7], we obtain: $\kappa = \sqrt{2(2m)U_{cp}}/\hbar$, which is simply the decay length for a particle of mass $2m$ to penetrate into a potential barrier U_{cp} at zero incident energy. Just as current density J can be written in terms of probability flux density for the Cooper pair wavefunction, we can also write the fluxon current density E in terms of the fluxon wavefunction. The use of the 1D wavefunction $u = \sqrt{r}\psi_\Phi$ and the extra factor of 2π for the PSJ in eq. 4 arise from the fact that fluxons are treated mathematically as one-dimensional objects [8], whose probability flux is only conserved when integrated around the azimuthal angle.

II. TYPE I PHASE SLIPS

Figure 1 illustrates a type I phase slip as discussed in the text. The type I limit where $\lambda_E \ll \xi$ can be viewed in the following way: λ_E is the length of wire whose kinetic series capacitance $\mathcal{C}_k/\lambda_E$ equals its shunt capac-

itance $\mathcal{C}_\perp \lambda_E$. In a type I or type II phase slip, This is effectively the length of wire necessary to hold the charge that flows onto and off of the core's series capacitance $\mathcal{C}_k \xi$ during a phase slip (passage of a fluxon through the wire). In the type I limit, this charging length becomes negligible and drops out of the problem (except insofar as the charging of the core boundaries is still required to drive the dynamics of the phase evolution). In this limit we find that a picture emerges which is different from the original intuition of Mooij and co-workers [3] that QPS involves tunneling through the same barrier that the wire passes over classically during an LAMH (type I) phase slip. Instead, in our theory, the type I phase slip is real penetration of a single fluxon through an observable, localized null in the order parameter, whereas a quantum phase slip is coherent (virtual) tunneling of a single fluxon through the entire wire, without suppression of the order parameter.

We can use this picture of type I phase slips to derive an intuitive result for the so-called "attempt rate" Ω that appears in the LAMH phase-slip resistance [1, 2, 4–6]:

$$R_{ps} = R_Q \frac{\hbar \Omega}{k_B T} \exp\left(-\frac{\Delta F}{k_b T} \right) \qquad (5)$$

Recall that the motion of Cooper pairs according to London's first equation can be described in terms a classical density n_s of charges $2e$ moving with velocity v and mass $2m$, using the relations: $\Lambda = 2m/n_s(2e)^2$ and $J = n_s 2ev$. Based on the picture above, we treat type I phase slips as classical, moving fluxons with kinetic energy described by $\hat{Q}^2/2\epsilon A$ [c.f. eq. 10 in the text], a one-dimensional density $n_\phi = 1/\xi$, and mass $m_\phi = \pi\epsilon\Phi_0^2/\xi$, such that $\epsilon \equiv m_\phi/n_\phi\Phi_0^2$ and $E = \Phi_0 n_\phi v_\phi/R$. It is easily verified that with these choices, the kinetic energy density then reduces to the classical 1D electrostatic energy density: $n_\phi m_\phi v_\phi^2/2 = (E^2/2\epsilon) \cdot A$. We can also rewrite $m_\phi \equiv (\epsilon B_\phi^2) \cdot A\xi$ with $B_\phi \equiv \Phi_0/R\xi$, such that the effective mass of a single fluxon is exactly what we would classically associate with a flux Φ_0 in the $\hat{\phi}$ direction contained inside a length ξ of the wire. We can estimate the thermal activation rate of these fluxons over an energy barrier ΔF for a wire of length l using the simple classical expression:

$$\Gamma = \frac{n_\phi v_\phi l}{R} \exp\left(\frac{-\Delta F}{k_B T} \right). \qquad (6)$$

To obtain a thermal average for v_ϕ, we use: $k_B T/2 = m_\phi \langle v_\phi^2 \rangle/2$, which results in:

$$\Omega = \frac{l}{\xi} \frac{V_\xi}{\Phi_0} \qquad (7)$$

where $V_\xi \equiv \sqrt{k_B T/C_\xi}$ is the root mean square thermal voltage at temperature T across $C_\xi \equiv \epsilon A/\xi$, the *series* capacitance of a length ξ of the wire. Equation 7 expresses the intuitive conclusion that the average attempt rate is simply the incoherent sum of thermal capacitive phase fluctuations across l/ξ segments of wire, each of length ξ. Note that this does not include the distributed *shunt* capacitance $C_\perp$ which is associated with fields outside the wire.

III. DETAILS ON THE ANALOG TO GIBBS FREE ENERGY

For a superconductor subjected to an external magnetic field $\mathbf{H}_e$, the thermodynamics of the field penetration is governed by a Gibbs free energy $G = F - V\mathbf{H}_e \cdot \mathbf{B}$, where F is the Helmholtz free energy and $\mathbf{B}$ is the actual magnetic flux density [7]. The Gibbs free energy accounts for the fact that the external flux source must do work if the flux is excluded from some or all of the superconductor (since it is effectively energizing a smaller inductance). It is used to describe the different type of flux penetration in type I and type II materials in terms of
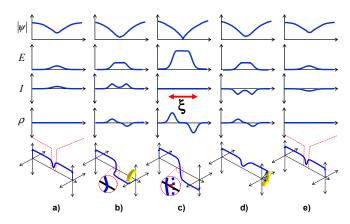

FIG. 1: Type I phase slips. The superconducting gap is suppressed in an area with dimension ξ (length $\sim \xi$ in the x direction and duration $\sim \xi/c_s$ in time), inside which a region of finite electric field exists. Screening "currents" $\mathbf{j}$ of width $\sim \lambda_E \ll \xi$ flow around this region of nonzero flux, just as in the 2D magnetic case. This process is none other than an LAMH phase slip. Panels (a)-(e) show snapshots in time of the evolution. First, a normal region of spatial size ξ begins to appear (a); then, current begins to flow, charging up C_k on the spatial boundaries of this region (b). This produces a local electric field which results in a winding (or unwinding) of the phase inside the fluctuation region, until the LAMH saddle point is reached [1, 2] and the current passes through zero (c); The current goes through zero and reverses, discharging C_k on the boundaries (d), until the system returns towards the uniform state (e). The net result is a single Φ_0 "slip" in the fluxoid across the wire. Note that unlike type II phase slips (Fig. 4 in the text), all of the dynamics occurs within a length ξ.

a surface energy of the interface between normal regions where the flux penetrates and superconducting regions where it is excluded (positive for type I, and negative for type II).

In our present 1+1D system, the most direct analog to the magnetic case just discussed would be an "electric flux" bias. The example of fig. 1(c) in the text, where an electric field is produced by magnetic flux in a moving frame, illustrates this. The additional term in the Euclidean action (eq. 15 in the text) associated with work done by the source can be written as:

$$S_{ext} = -\int \left(\frac{\mathbf{E}_{ext}}{c_s} \right) \cdot \mathbf{d}\, da \qquad (8)$$

and can be understood as arising from the mechanical work required to maintain the motion of the magnetic source. Analogous arguments can be made about the surface energy of normal and superconducting regions: for example, in the time dimension, for type I electric flux penetration (LAMH phase slips), the order parameter is *first* suppressed before any currents flow, such that the source does not provide any energy; for type II phase slips, a fluxoid of $\Phi_0/2$ has already appeared across the source before the gap begins to decrease near the core.

Wire	A [nm^2]	I_{sw} [μA]	T_C [K]	B_C [mT]	L_k [nH]	E_L [THz]	E_S [GHz]
S1	74	2.37	3.9	67	1.1	2.9	170
S2	86	1.4	3.8	66	1.7	1.9	140
S3	130	1.42	3.2	61	0.73	4.5	7.0
S4	92	0.91	2.9	58	2.2	1.5	180
S5	150	4.9	4.6	73	0.51	6.3	0.48

TABLE I: MoGe wire parameters used in figs. 5(e)-(f). For all wires we use $\rho_n = 1.8$ $\mu\Omega\cdot$m from ref. 6, $\xi = 4.5$ nm from ref. 26 and $\epsilon = 25\epsilon_0$ and $a = 0.21$ which give a reasonable fit to the data in fig. 5(f) of the text. For fig. 5(e) of the text we obtain $R_{hf} = 115\Omega$ from the linear fit shown, with $C_{sh} = 1$ fF.

As the gap goes to zero and the phase evolution along the wire is concentrated into a region of length ξ [figs. 4(b)-(c)], the effective inductance of the wire (seen by the source) is changing while the source is providing nonzero Φ, such that the source provides energy. Analogs to the usual results for flux penetration follow from this, for example: a lower critical electric field below which an electric Meissner effect would exclude $\mathbf{E}_{ext}$, and above which an Abrikosov lattice of type II phase slips would form [7].

Experimentally, the wires are biased with an external voltage or current source, rather than electric "flux". This case can be described by:

$$\mathcal{S}_{ext} = -\int \left(\frac{\mathbf{J}_{ext}}{c_s} \right) \cdot \mathbf{j} \, da \qquad (9)$$

where $\mathbf{J}_{ext} \equiv I_s\hat{\mathbf{x}} + V_s/Z_L\hat{\mathbf{y}}$ with I_s and V_s the current through and voltage across the external source, respectively. Equation 9 describes work done by the source when either: (i) the effective inductance of the wire changes while the source is supplying a given current; or (ii) when the effective series capacitance of the wire changes while the source is supplying a given voltage. This expression reduces to that used in ref. 11 when the contribution from V_s can be neglected, and for a fixed source current.

IV. DETAILS ON CALCULATIONS AND PARAMETER VALUES

Table I lists the parameters used in our calculations for wires S1-5 in ref. 6 (fig. 5(g) and (h) in the text). These values are taken from the supplementary material of ref. 6, except for the coherence length ξ, which we take from ref. 26. The values listed for ξ in ref. 6 were obtained only indirectly through fits to LAMH phase slip rates, and varied rather widely, from 5-12 nm.

To obtain the inductive energy E_L, we calculate the Ginzburg-Landau (GL) penetration depth λ from the sheet resistance using the dirty-limit relation:

$$\frac{\Lambda}{\rho_n} = a\frac{\hbar}{k_B T_C} \qquad (10)$$

where $\Lambda = \mu_0\lambda^2$, ρ_n is the normal-state resistivity, and a is a numerical constant [9]. The inductive energy is given by:

$$E_L = \frac{\Phi_0^2}{2L_k} = \frac{\Phi_0^2 A}{2\mu_0\lambda^2 l} \qquad (11)$$

To calculate the condensation energy U_C, we use the value for λ and the GL coherence length ξ in table I, along with the GL result for the thermodynamic critical field:

$$B_C = \frac{\Phi_0}{2\pi\sqrt{2}\lambda\xi} \qquad (12)$$

We then have $U_C = B_C^2/2\mu_0$. This value is used to calculate E_C:

$$E_C = \sqrt{\frac{2U_C}{\epsilon}}\frac{1}{2\pi\kappa_\Phi R[K_0(\kappa_\Phi R)^2 + I_0(\kappa_\Phi R)^2]} \qquad (13)$$

$$\approx \sqrt{\frac{2U_C}{\epsilon}}\exp(-2\kappa_\Phi R), \quad \kappa_\Phi R \ll 1 \qquad (14)$$

where K_0 and I_0 are the modified Bessel functions, and $\kappa_\Phi R$ is given in eq. 3. Note that although eq. 14 comes from the exact solution to the Schrödinger equation at zero energy for all $\kappa_\Phi R$, the use of that equation is itself only an approximation which may break down for small $\kappa_\Phi R$. Just as in the macroscopic quantum model of a JJ, the use of a Schrödinger-like equation inside the barrier is based on the approximation that interactions between fluxons (Cooper pairs for a JJ) can be neglected in that region. This approximation also underlies the description of the phase-slip and Josephson potentials [10]:

$$\hat{U}_{JJ} = -E_J \cos\hat{\phi} = -\frac{1}{2}(e^{i\hat{\phi}} + e^{-i\hat{\phi}}) = -\frac{E_J}{2}\sum_n (|n+1\rangle\langle n| + |n-1\rangle\langle n|) \tag{15}$$

$$\hat{U}_{PSJ} = -E_S \cos\hat{q} = -\frac{1}{2}(e^{i\hat{q}} + e^{-i\hat{q}}) = -\frac{E_S}{2}\sum_m (|m+1\rangle\langle m| + |m-1\rangle\langle m|) \tag{16}$$

where on the right only terms which transfer one fluxon or Cooper pair through the junction are included.

The calculated quantum temperature shown in fig. 5(g) of the text is associated with the zero-point fluctuations of the resonant circuit formed by the kinetic inductance of the wire L_k and the lumped shunt capacitance of the environment C_{sh}, and is given by [12]:

$$\hbar\omega_Q = \hbar\omega_0\left[\sqrt{1 + \frac{1}{(2\omega_0\tau)^2}} - \frac{1}{2\omega_0\tau}\right] \approx \hbar\frac{R_{hf}}{L_k} \tag{17}$$

where $\tau = R_{hf}C_{sh}$ and $\omega_0 = 1/\sqrt{L_k C_{sh}}$. The approximate equality holds in the overdamped limit $\omega_0\tau \ll 1$, which is well satisfied for the wires of ref. 6 for $R_{hf} \sim 100\Omega$ and $C_{sh} \sim$1-10 fF.

To calculate the predicted switching currents I_{sw} shown in fig. 5(h) of the text, we start with the classical energy $U(I_b, \Phi_e) = U_0(\Phi_e) - I_b\Phi_0$ of the lowest band shown in fig. 5(c), for a fixed fluxoid Φ_e across the wire, and a fixed current bias I_b. The calculation of $U_0(\Phi_e)$ is formally equivalent to the finding the energies of the phase-slip qubit [9], where in that case the phase bias is supplied via an external flux Φ_e through the closed loop. To calculate the energy levels, we diagonalize the Hamiltonian:

$$\hat{H}(\Phi_e) = E_L\left(\frac{\hat{\Phi} - \Phi_e}{\Phi_0}\right)^2 - E_S\cos\left(\frac{\hat{Q}}{Q_0}\right) \tag{18}$$

where $[\hat{Q}, \hat{\Phi}] = i\hbar$. We use a discrete fourier grid representation in fluxon states $\langle\hat{q}|m\rangle = \exp(im\hat{q})$ which yields $U_n(\Phi_e)$ numerically. An example of the resulting potential energy for wire S1 as a function of Φ_e is shown in figs. 5(e)and (f) of the text. Quantum fluctuations of Φ at zero temperature about the classical minimum-energy equilibrium value, given by eq. 17 above, are also shown. We take the average switching current at which the phase particle escapes the potential well to be that at which the potential well depth is equal to T_Q. This condition is used to obtain the predicted I_{sw} vales shown in fig. 5(h) of the text.

Table II shows the parameter values used for the plots in fig. 6 of the text. For the Giordano [4] and GZ [13] results in Figs. 6(b) and (a), we used:

Material	t [nm]	ξ [nm]	T_C [K]	$R_\square$ [Ω]	ϵ [ϵ_0]	B_C [mT]	Refs
$Nb_{0.15}Si_{0.85}$	12.5	58	0.21	1400	110	0.48	[17, 18]
$Nb_{0.45}Si_{0.55}$	10	5	1.2	550	110	24	[9, 18, 19]
TiN	5	10	2	4200	30	7.8	[20, 21]
InO_x	20	6	1.5	3500	20	6.2	[22–24]
InO_x	35	10	2.7	1600	20	5.4	[24, 25]
In	42	52	4.2	2.9	20	28	[4]
$Mo_{0.79}Ge_{0.21}$	8.6	4.5	3.9	210	25	67	[6, 26]

TABLE II: Material parameters used in Fig. 6.

$$E_S^{gio} = 1.5\frac{l}{\xi}\sqrt{\frac{R_Q}{R_\xi}}\frac{k_B T_C}{\hbar}\exp\left(-0.3\frac{R_Q}{R_\xi}\right) \tag{19}$$

$$E_S^{GZ} = 1.8\frac{l}{\xi}\frac{R_Q}{R_\xi}\frac{k_B T_C}{\hbar}\exp\left(-\frac{R_Q}{R_\xi}\right) \tag{20}$$

where in both cases we have taken unknown numerical factors of order unity to be 1.

V. CONNECTION TO JJ ARRAYS

The model we have described for QPS, in which the quantum fluctuations that allow fluxon tunneling arise from an effective mass for the phase which is associated with the permittivity ϵ, is conceptually linked to earlier work on 1D JJ arrays as well as the work of Glazman and co-workers in which QPS in a wire was *modeled* using a 1D JJ array [27]. in fact, one might view our model as a continuum version of a 1D JJ array, in the sense that such an array consists of alternating domains of purely real and purely imaginary permittivity (the insulating barriers, and superconducting islands, respectively) whereas we combine the two into a continuous medium with complex permittivity. This connection can be illustrated by re-casting our result for the phase-slip energy E_S in the following form (using eq. 12):

$$E_S \approx \frac{l}{\xi}\sqrt{2V_L V_C}\exp\left[-\sqrt{\frac{2V_L}{V_C}}\right], \qquad \frac{V_L}{V_C} \gg 1$$

$$V_L = \frac{\bar{\Phi}_0^2}{2L_\xi} \quad V_C = \frac{\bar{Q}_0^2}{2C_\xi} \tag{21}$$

where $L_\xi = \Lambda\xi/A$ and $C_\xi \equiv \epsilon A/\xi$ are the kinetic inductance and series capacitance, respectively, of a fluctuation volume $\tau_\xi = \xi \cdot A$. The quantity V_L is the 1D analog of the so-called "superfluid stiffness", defined in a bulk superconductor for $\tau_\xi = \xi \cdot \xi \cdot \xi$ [16], which describes the potential energy cost (the spring constant) for phase fluctuations. We then associate V_C with a kinetic energy (effective mass) of those fluctuations. Equation 21 is nearly identical to the result for the width of the lowest quasicharge band in a 1D JJ array (e.g., ref. 27), with V_L playing the role of the Josephson energy E_J, V_C playing the role of the charging energy E_C, and l/ξ playing the role of the number of junctions in the array.

The electric penetration depth λ_E also has an analog in the physics of JJ arrays. In that case, there is an electric screening length given by: $\lambda_c = \sqrt{C/C_0}$ (in units of the lattice constant of the array) [28], where C is the junction barrier capacitance, and C_0 is the shunt capacitance to ground (or to a low-Z bias source) of each superconducting island. This is essentially identical to our result for a distributed PSJ (eq. 18 in the text), with the barrier capacitance suitably replaced with the kinetic capacitance.

VI. ALTERNATIVE EXPLANATION OF GIORDANO'S RESULTS

Figure 2 shows how the present theory may explain the resistance "tails" observed by Giordano, which have been interpreted as direct evidence for QPS [4]. The blue line shows our result for the LAMH resistance, where we have used the same result for the barrier height as Giordano (the LAMH expression scaled by a factor of 1/4 [4]) and our result from eq. 7 for the prefactor. For the red line in the plot we have used eq. 5, but with an energy barrier of $\Delta F = E_L/4$, and an attempt rate of:

$$\Omega_l \equiv \frac{V_l}{\Phi_0} \qquad (22)$$

where $V_l \equiv \sqrt{k_B T/C_{sh}}$ is the rms thermal voltage across C_{sh}, for which we have used $C_{sh} \sim l\epsilon_{eff} \sim 5$ fF (where $l = 80\mu$m is the wire length and $\epsilon_{eff} \sim 5\epsilon_0$ is the average permittivity of the surrounding media). We have used the results of ref. [6] for the temperature dependence of relevant parameters. The dotted lines indicate where each result is no longer valid. This plot compares favorably to figure 1 in Ref. [4].

VII. PSJ CIRCUITS

Figure 3 shows specific examples of flux-charge duality applied to more complicated JJ-based circuits. Panels (a) and (b) show the duality between a charge qubit and the phase-slip qubit of ref. 9. PSJ-based superconducting qubits may be of particular interest since flux and
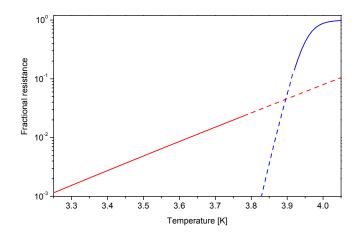

FIG. 2: Resistance tails of Giordano and type II phase slips. The asymptotic prediction for $\lambda_E \gg l$ is shown in red, and our LAMH prediction in blue. No fitting parameters were adjusted, although we did retain Giordano's factor of 1/4 in the LAMH energy barrier [4]. The temperature dependence of all quantities was taken from the supplementary information of ref. 6.

charge noise will have their roles interchanged relative to JJ-based qubits. Since the excited-state lifetimes of present-day JJ-based qubits are thought to be limited by high-frequency charge noise, exchanging this for high-frequency flux noise (which is thought to be much weaker [29]) should result in much longer lifetimes. Panels (a) and (b) also illustrate how polarization charge on the nanowire (produced by a nearby gate electrode) is dual to magnetic flux *through* the junction barrier of the JJ. Just as a Fraunhofer interference pattern will be observed in the magnitude of E_J vs. flux through the junction (due to the Aharanov-Bohm effect) [7], the same pattern will be observed in the magnitude of E_S vs. charge on the nanowire (due to the Aharanov-Casher effect [8]). This may be important for the phase-slip qubit since it implies charge noise on the nanowire would show up as V_C noise in the qubit (dual to I_C noise commonly observed in JJ-based qubits [30]). Panels (c)-(f) show two tunable superconducting qubits and their dual circuits. Just as a DC SQUID can be used to implement a flux-tunable composite JJ, the series combination of two PSJs as shown can be used to implement a charge-tunable composite PSJ. Note that (d) is essentially a tunable version of the phase-slip oscillator of Ref. [31], and (f) is a tunable version of the phase-slip qubit [9].

In addition to qubits, where well-defined, long-lived energy eigenstates are required in which quantum zero-point fluctuations must be kept undisturbed by the environment, the circuits shown in (g)-(l) are intended to function in a regime where either fluxoid (for JJs) or quasicharge (for PSJs) is a *classical* variable (i.e. where quantum fluctuations are small). A well-defined fluxoid requires a low environmental impedance at the Josephson plasma frequency, which is readily obtained using resistively shunted Josephson junctions. A well-defined
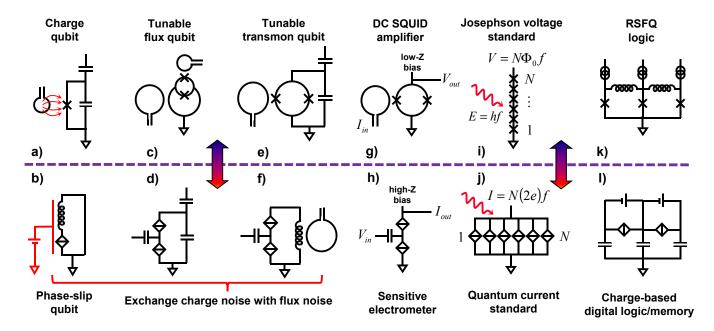
FIG. 3: Dual circuits for some well-known JJ devices.

quasicharge requires a *high* environmental impedance ($\gg R_Q$) at the phase-slip plasma frequency, which is much more difficult to realize. In ref. 19, highly-resistive Cr nanowires were used to bias the device; in ref. 32, frustrated DC SQUID arrays in an insulating state were used. Panel (h) shows the "quantum phase slip transistor" QPST, first suggested in ref. 33, and implemented in ref. 19. This device is an electrometer, dual to the DC SQUID amplifier shown in (g). The QPST is similar to a single Cooper-pair transistor (SCPT) [34]; however, it could have a much higher sensitivity than an SCPT, which is limited by the charging energy of the JJs (by how small one can make the junction capacitance). The QPST is instead limited by the kinetic capacitance C_k, whose ultimate limit is the *series* capacitance of the wires, which can be much smaller. Panel (i) is the Josephson voltage standard, and (j) the quantum current standard proposed in ref. [10]. Under microwave irradiation, dual features to Shapiro steps would allow locking of the incident frequency f to the applied current I according to $I = Nf2e$, where N is the number of parallel PSJs. Such a device would have enormous impact in electrical metrology, allowing for the first time interconnected fundamental standards of voltage, resistance, and current [35]. Finally, panel (k) is a Josephson transmission line, a basic building block of rapid single flux quantum (RSFQ) digital logic; (l) shows the dual to this, in which shunt JJs are replaced by series PSJs, flux stored in loops is replaced by charge stored on islands, and current bias is replaced by voltage bias. Such circuits could be of great practical interest, both because unlike RSFQ they have no static power dissipation, and also because voltage-state logic could be significantly easier to integrate with memory elements than flux-state logic.

VIII.   TABLES OF VARIABLES

Quantity	value	units	description	Quantity	value	units	description
Q		C	quasicharge	Φ		V·s	fluxoid
$\mathbf{J}_Q$		A·s^{-1}	quasicharge current density	$\mathbf{J}_\Phi$		V·m^{-1}	fluxoid current density (electric field)
I		A	current	V		V	electric potential
J		A·m^{-2}	current density	E		V·m^{-1}	electric field
ρ_Q		C·m^{-3}	free charge density	$\mathbf{B}_f$		T	free flux density
$\mathbf{v}_Q$		m·s^{-1}	free quasicharge velocity	$\mathbf{v}_\Phi$		m·s^{-1}	free fluxoid velocity
Λ	$\mu_0 \lambda^2$	H·m	London coefficient (kinetic inductivity)	ϵ		F·m^{-1}	real part of electric permeability (bound charge only)
n		-	number of Cooper pairs that have tunneled through a JJ	m		-	number of fluxons that have tunneled through a PSJ
C_J		F	shunt capacitance of JJ electrodes	L_k		H	series kinetic inductance of PSJ
A_{JJ}		m^2	total area of a JJ	l		m	total length of a wire
Φ_0	$h/2e$	V·s	superconducting flux quantum	$2e$		C	superconducting charge quantum
Φ_0	$\hbar/2e$	V·s	reduced superconducting flux quantum	Q_0	$2e/2\pi$	V·s	reduced superconducting charge quantum
$\hat{T}^Q_{2D}$	$\hat{\Phi}^2/2\mathcal{L}_A$	J·m^{-2}	2D kinetic energy density of a JJ	$\hat{T}^\Phi_{1D}$	$\hat{Q}^2/2\mathcal{C}_l$	J·m^{-1}	1D kinetic energy density of a PSJ
$\hat{U}^Q_{2D}$	$n_s d U_{cp}$	J·m^{-2}	2D potential energy density of a JJ	$\hat{U}^\Phi_{1D}$	$U_C A$	J·m^{-1}	1D potential energy density of a PSJ
ψ_Q		m$^{-3/2}$	macroscopic wavefunction for Cooper pairs inside JJ barrier	ψ_Φ		m$^{-3/2}$	macroscopic wavefunction for fluxons inside superconductor
κ_Q		m^{-1}	Decay coefficient for ψ_Q inside JJ barrier	κ_Φ		m^{-1}	Decay coefficient for ψ_Φ inside superconductor
J_C		A·m^{-2}	critical current density for a JJ	E_C		V·m^{-1}	critical electric field for a PSJ
E_J	$\Phi_0 J_C A_{JJ}$	J	Josephson energy for a JJ	E_S	$Q_0 E_C l$	J	phase-slip energy for a PSJ
E_C	$(2e)^2/2C_J$	J	charging energy for a JJ	E_L	$\Phi_0^2/2L_k$	J	inductive energy for a PSJ
λ_J	$\sqrt{\frac{\Phi_0}{J_C \mathcal{L}_\square}}$	m	Josephson penetration length	λ_E	$\sqrt{\frac{Q_0}{E_C \mathcal{C}_\perp}}$	m	electric penetration length
$L_\square$		H	geometric sheet inductance of JJ barrier	$\mathcal{C}_\perp$		F·m^{-1}	shunt capacitance per length of wire
$\mathcal{C}_{JJ}$		F·m^{-2}	specific capacitance of JJ barrier	$\mathcal{L}_k$		H·m^{-1}	kinetic inductance per length of PSJ
L_{J0}	$\Phi_0/J_C A_{JJ}$	H	Josephson inductance for a JJ	C_{k0}	$Q_0/E_C l$	F	kinetic capacitance for a PSJ
ω_p	$\sqrt{1/L_{J0}C_J}$	s^{-1}	Josephson plasma frequency	ω_p	$\sqrt{1/LC_{k0}}$	s^{-1}	phase slip plasma frequency
$U_{cp}n_s$		J·m^{-3}	potential energy density for Cooper pairs inside JJ barrier	U_C	$\frac{B_C^2}{2\mu_0}$	J·m^{-3}	condensation energy

TABLE III: Selected parameters and their duals.

[1] W.A. Little, *Decay of persistent currents in small superconductors*, Phys. Rev. **156**, 396 (1967).

[2] J.S. Langer and V. Ambegaokar, *Intrinsic resistive transition in narrow superconducting channels*, Phys. Rev. **164**, 498 (1967); D.E. McCumber and B.I. Halperin, *Time scale of intrinsic resistive fluctuations in thin superconducting wires*, Phys. Rev. B **1**, 1054 (1970).

[3] A.J. van Run, J. Romijn, and J.E. Mooij, *Superconducting phase coherence in very weak aluminium strips*, Jpn. J. Appl. Phys. Supplement 26-3-2, 1765 (1987).

[4] N. Giordano, *Evidence for macroscopic quantum tunneling in one-dimensional superconductors*, Phys. Rev. Lett. **61**, 2137 (1988).

[5] C.N. Lau, N. Markovic, M. Bockrath, A. Bezryadin, and M. Tinkham, *Quantum phase slips in superconducting nanowires*, Phys. Rev. Lett. **87**, 217003 (2001)

[6] M. Sahu, M.-H. Bae, A. Rogachev, D. Pekker, T.-C. Wei, N. Shah, P.M. Goldbart, and A. Bezryadin, *Individual topological tunnelling events of a quantum field probed through their macroscopic consequences*, Nature Physics **5**, 506 (2009).

[7] T.P. Orlando and K.A. Delin, *Foundations of Applied Superconductivity*, Addison-Wesley, 1991.

[8] D. Rohrlich, *Duality in the Aharonov-Casher and Aharonov-Bohm effects*, J. Phys. A 43, 354028 (2010).

[9] J.E. Mooij and C.J.P.M. Harmans, *Phase-slip flux qubits*, N. J. Phys. **7** 219 (2005).

[10] J.E. Mooij and Yu.V. Nazarov, *Superconducting

Quantity	value	units	description
ξ		m	Ginsburg-Landau coherence length
T_C		K	mean-field critical temperature
R_Q	$h/4e^2$	Ω	Cooper pair resistance quantum
R_n		Ω	total normal-state resistance
λ		m	Ginsburg-Landau magnetic penetration depth
n_s		m^{-3}	Cooper pair density
m		kg	electron mass
U_{cp}		J	effective Cooper pair potential energy inside insulator
$\mathcal{P}$	$\epsilon \mathbf{E} \times \mathbf{B}$	$kg \cdot m^{-2} \cdot s^{-1}$	electromagnetic momentum density
ρ_Φ	$\epsilon \mathbf{B}^2$	$kg \cdot m^{-3}$	effective mass density for moving flux
R		m	radius of a wire
d		m	thickness of a JJ barrier
A		m^2	cross-sectional area of a wire
B_C	$\frac{\Phi_0}{2\pi\sqrt{2}\lambda\xi}$	$V \cdot s \cdot m^-2$	thermodynamic critical field
$E_{S\lambda}$	$\frac{\bar{Q}_0^2}{\mathcal{C}_\perp \lambda_E}$	J	phase-slip energy for a PSJ with wire length equal to λ_E

TABLE IV: Additional parameters defined in the text.

nanowires as quantum phase-slip junctions, Nature Physics **2**, 169 (2006).

[11] H.P. Büchler, V.B. Geshkenbein, and G. Blatter, *Quantum fluctuations in thin superconducting wires of finite length*, Phys. Rev. Lett. **92**, 067007 (2004).

[12] H. Grabert and U. Weiss, *Crossover from thermal hopping to quantum tunneling*, Phys. Rev. Lett. **53**, 1787 (1984).

[13] A.D. Zaikin, D.S. Golubev, A. van Otterlo, G.T. and Zimányi, *Quantum phase slips and transport in ultrathin superconducting wires*, Phys. Rev. Lett. **78**, 1552 (1997); D.S. Golubev and A.D. Zaikin, *Quantum tunneling of the order parameter in superconducting nanowires*, Phys. Rev. B **64**, 014504 (2001).

[14] J.M. Martinis, M.H. Devoret, and J. Clarke, *Experimental tests for the quantum behavior of a macroscopic degree of freedom: The phase difference across a Josephson junction*, Phys. Rev. B **35**, 4682 (1987)

[15] R.L. Kautz and J.M. Martinis, *Noise-affected I-V curves in small hysteretic Josephson junctions*, Phys. Rev. B **42**, 9903 (1990).

[16] V.J. Emery and S.A. Kivelson, *Importance of phase fluctuations in superconductors with small superfluid density*, Nature **374**, 434 (1995).

[17] C.A. Marrache-Kikuchi, H. Aubin, A. Pourret, K. Behnia, J. Lesueur, L. Bergé, and L. Dumoulin, *Thickness-tuned superconductor-insulator trnasitions under magnetic field in a-NbSi*, Phys. Rev. B **78**, 144520 (2008).

[18] E. Helgren, G. Grüner, M.R. Ciofalo, D.V. Baxter, and J.P. Carini, *Measurements of the complex conductivity of Nb_xSi_{1-x} alloys on the insulating side of the metal-insulator transition*, Phys. Rev. Lett. **87**, 116602 (2001).

[19] T.T. Hongisto and A.B. Zorin, arXiv:1109.3634.

[20] T.I. Baturina, A.Y. Mironov, V.M. Vinokur, M.R. Baklanov, and C. Strunk, *Localized superconductivity in the quantum-critical region of the disorder-driven superconductor-insulator transition in TiN thin films*, Phys. Rev. Lett. **99**, 257003 (2007)

[21] T.I. Baturina, J. Bentner, C. Strunk, M.R. Baklanov, and A. Satta, *From quantum corrections to magnetic-field-tuned superconductorinsulator quantum phase transition in TiN films*, Physica B **359**, 500 (2005).

[22] G. Sambandamurthy, L.W. Engel, A. Johansson, and D. Shahar, *Superconductivity-related insulating behavior*, Phys. Rev. Lett. **92**, 107005 (2004).

[23] M. Steiner and A. Kapitulnik, *Superconductivity in the insulating phase above the field-tuned superconductorinsulator transition in disordered indium oxide films*, Physica C **422**, 16 (2005).

[24] O. Entin-Wohlman and Z. Ovadyahu, *Modifications of hopping transport due to electrostatically enhanced coulomb repulsion*, Phys. Rev. Lett. **56**, 643 (1986).

[25] Astafiev, O., Private communication.

[26] G.M. Graybeal and M.R. Beasley, *Localization and interaction effects in ultrathin amorphous superconducting films*, Phys. Rev. B **29**, 4167 (1984).

[27] K.A. Mateev, A.I. Larkin, and L.I. Glazman, *Persistent current in superconducting nanorings*, Phys. Rev. Lett. **89**, 096802 (2002).

[28] T.P. Orlando, J.E. Mooij, H.S.J. van der Zant, *Phenomenological model of vortex dynamics in arrays of Josephson junctions*, Phys. Rev. B **43**, 10218 (1991).

[29] A.J. Kerman, *Metastable superconducting qubit*, Phys. Rev. Lett. **104**, 027002 (2010).

[30] D.J. van Harlingen, T.L. Robertson, B.L.T. Plourde, P.A. Reichardt, T.A. Crane, and J. Clarke, *Decoherence in Josephson-junction qubits due to critical-current fluctuations*, Phys. Rev. B **70**, 064517 (2004).

[31] A.M. Hriscu and Yu.V. Nazarov, *Model of a proposed superconducting phase slip oscillator: a method for obtaining few-photon nonlinearities*, Phys. Rev. Lett. **106**, 077004 (2011).

[32] S. Corlevi, W. Guichard, F.W.J. Hekking, and D.B. Haviland, *Phase-charge duality of a Josephson junction in a fluctuating electromagnetic environment*, Phys. Rev. Lett. **97** 096802 (2006).

[33] A.M. Hriscu and Yu.V. Nazarov, *Coulomb blockade due to quantum phase slips illustrated with devices*, Phys. Rev. B **83**, 174511 (2011).

[34] A.B. Zorin, S.V. Lotkhov, Yu.A. Pashkin, H. Zangerle, V.A. Krupenin, T. Weimann, H. Scherer, and J. Niemeyer, *Highly sensitive electrometers based on single Cooper pair tunneling*, J. Supercond. **12**, 747 (1999).

[35] J. Flowers, *The route to atomic and quantum standards*, Science **306**, 1324 (2004).

[36] B.J. van Wees, *Duality between Cooper-pair and vortex dynamics in two-dimensional Josephson-junction arrays*, Phys. Rev. B **44**, 2264 (1991).

[37] W. Skocpol, M.R. Beasley, and M. Tinkham, *Phase-slip centers and nonequilibrium processes in superconducting tin microbridges*, J. Low Temp. Phys. **16**, 145 (1974).